Available on CMS information server

CMS NOTE 2000/017

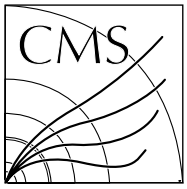

The Compact Muon Solenoid Experiment

CMS Note

Mailing address: CMS CERN, CH-1211 GENEVA 23, Switzerland

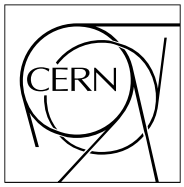

Sensitivities for anomalous WWγ and ZZγ couplings at CMS

Th. Müller, D. Neuberger[a)], W.H. Thümmel

Institut für Experimentelle Kernphysik, Universität Karlsruhe

Abstract

We have investigated sensitivities on non-Standard Model WWγ and ZZγ couplings using the Wγ and Zγ NLO event generators by Baur et al. in conjunction with a realistic CMS detector simulation. Performing a likelihood fit to the distribution of the photon transverse momentum, which is most sensitive to Standard Model deviations, yields compared to present results greatly improved sensitivities at energy scales up to $10\,\mathrm{TeV}$.

[a)] *corresponding author; email: neuberg@ekp.physik.uni-karlsruhe.de*

1 Introduction

Gauge boson self-interactions are well described within the framework of the Standard Model. From the possible triple boson vertices WWγ, WWZ, ZZγ, Z$\gamma\gamma$, and ZZZ[1)], only the first two are allowed at tree level. In recent years, experiments at the Tevatron and at LEPII have obtained first information about these couplings through the analysis of diboson production [1–5].

Although most fermion-vector boson interactions are measured today with precisions of less than 1%, our knowledge of triple-gauge couplings remarkably lags behind. Measurements of diboson couplings at LEPII and the Tevatron carry uncertainties in the order of 10-50%. The LHC experiments will change this situation dramatically. As the diboson cross section grows with the center-of-mass energy at hadron colliders, and integrated luminosities up to 100 fb^{-1}/year are expected, large amounts of gauge-boson pairs will be available at CMS and ATLAS. It will be possible to perform precision measurements which will either confirm the gauge theory structure of the trilinear vertex or give hints of deviations from the Standard Model.

In this paper, we investigate the question: how sensitive to WWγ and ZZγ couplings will the CMS experiment be?

2 WWγ and ZZγ couplings

Despite its incredible success, the Standard Model is believed to represent only the low-energy limit of a more fundamental theory. A model-independent effective Lagrangian is generally used to conveniently parameterize non-Standard Model effects. For example, the most general notation for the Wγ effective Lagrangian contains seven coupling parameters. The coupling of the W boson to essentially massless fermions and the gauge invariance of the on-shell photon restrict the choice to four parameters, which are commonly named λ and $\Delta\kappa$ for the $\mathcal{CP}$-conserving, and $\tilde{\lambda}$ and $\tilde{\kappa}$ for the $\mathcal{CP}$-violating WWγ couplings. While these parameters have no physical meaning as such, they are related to the electromagnetic moments of the W boson:

$$\mu_W = \frac{e}{2M_W}(2+\Delta\kappa+\lambda) \quad \text{Magnetic Dipole Moment,} \tag{1}$$

$$Q_W = -\frac{e}{M_W^2}(1+\Delta\kappa-\lambda) \quad \text{Electric Quadrupole Moment,} \tag{2}$$

$$d_W^e = \frac{e}{2M_W}(\tilde{\kappa}+\tilde{\lambda}) \quad \text{Electric Dipole Moment,} \tag{3}$$

$$Q_W^m = -\frac{e}{M_W^2}(\tilde{\kappa}-\tilde{\lambda}) \quad \text{Magnetic Quadrupole Moment,} \tag{4}$$

where $(\Delta\kappa = \kappa - 1) = \lambda = \tilde{\kappa} = \tilde{\lambda} = 0$ in the Standard Model. A measurement of a non-vanishing value for these couplings would hint at the existence of composite gauge bosons, novel interactions or other so-far unknown phenomena beyond a certain energy scale.

To avoid violation of partial wave unitarity at large center-of-mass energies, a unitarization method has to be applied to the effective Lagrangian. The traditionally preferred way is to replace the coupling parameters by form factors which fall off rapidly at an energy scale Λ. In analogy to nuclear physics, a generalized dipole shape with a cut-off value Λ is chosen for the form factor function:

$$a_f(M_{W\gamma}^2, q_1^2 = M_W^2, q_2^2 = 0) = \frac{a_0}{\left(1+\frac{M_{W\gamma}^2}{\Lambda^2}\right)^n} \quad ,$$

where q_1 and q_2 are the four momenta of the final state W boson and photon, respectively. This choice is, within the requirements, arbitrary and its interpretation is model-dependent. The true functional behavior can only be determined experimentally—when sufficient statistics is available. With the absence of an applicable theory, however, the dipole ansatz remains a simple and reasonable approach. All present experimental limits on anomalous couplings are published for a given form factor parameter set Λ and n. The lowest possible value for the WWγ couplings λ, $\Delta\kappa$, and $\tilde{\lambda}$ is $n = 1$, for $\tilde{\kappa}$ it is $n = 1/2$. For the ZZγ couplings h_{10}^Z, h_{20}^Z and h_{30}^Z, h_{40}^Z, the limit is $n = 3/2$ and $n = 5/2$, respectively. Lower values would lead to unitarity violations.

[1)] $\gamma\gamma\gamma$ is forbidden by electromagnetic gauge invariance

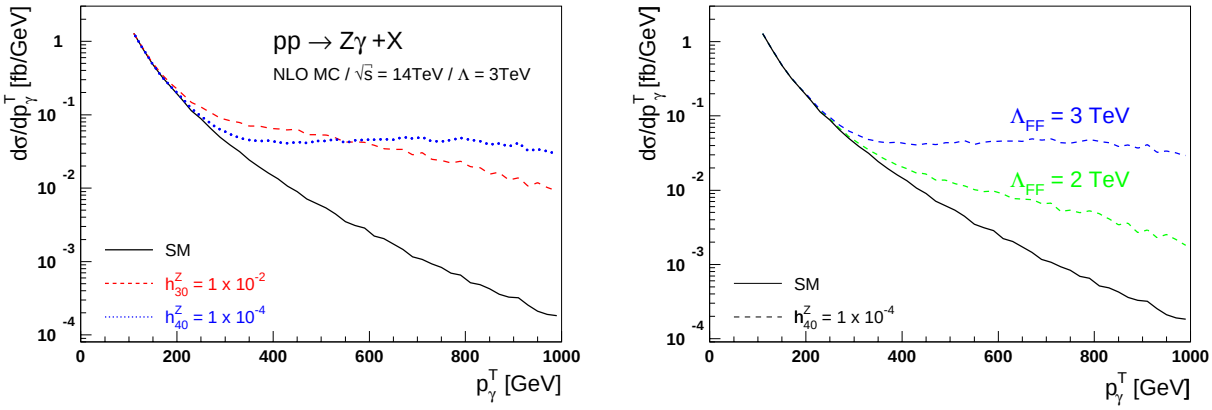

Figure 1: $pp \to Z\gamma + X$ cross section increases at high photon P_T in presence of anomalous couplings.

A remarkable feature of Standard Model Wγ production is that, due to gauge cancellations in all helicity amplitudes, the cross section vanishes at a particular value of the photon scattering angle [6]. This so-called radiation zero is partially eliminated in presence of anomalous WWγ couplings.

The ZZγ vertex is treated in close analogy to the WWγ vertex. The $\mathcal{CP}$-conserving couplings are named h_{30}^Z and h_{40}^Z, and the $\mathcal{CP}$-violating couplings h_{10}^Z and h_{20}^Z. As there are no static moments of the Z boson, these parameters relate to *transition moments* [7]:

$$d_{Z_T} = -\frac{e}{M_Z}\frac{1}{\sqrt{2}}\frac{k^2}{M_Z^2}(h_{30}^Z - h_{40}^Z) \quad \text{Electric Dipole Transition Moment,} \tag{5}$$

$$Q^e_{Z_T} = \frac{e}{M_Z^2}\sqrt{10}(2h_{10}^Z) \quad \text{Electric Quadrupole Transition Moment,} \tag{6}$$

$$\mu_{Z_T} = -\frac{e}{M_Z}\frac{1}{\sqrt{2}}\frac{k^2}{M_Z^2}(h_{10}^Z - h_{20}^Z) \quad \text{Magnetic Dipole Transition Moment,} \tag{7}$$

$$Q^m_{Z_T} = \frac{e}{M_Z^2}\sqrt{10}(2h_{30}^Z) \quad \text{Magnetic Quadrupole Transition Moment,} \tag{8}$$

where $h_{10}^Z = h_{20}^Z = h_{30}^Z = h_{40}^Z = 0$ in the Standard Model.

The Z$\gamma\gamma$ vertex is almost identical to the ZZγ vertex; one just has to replace the virtual Z boson by a photon. Because the sensitivities on both vertices are expected to be similar, we constrained our study to the ZZγ vertex.

Since the Z boson, being its own anti-particle, has no electric charge nor weak isospin, ZZγ and Z$\gamma\gamma$ vertices are CPT-violating in the Standard Model. Consequently, the detection of Zγ events coming from a ZZγ or Z$\gamma\gamma$ vertex would automatically signal evidence for the existence of new physics beyond the Standard Model.

The presence of anomalous couplings would lead to an enhanced cross section in boson pair production at high diboson masses. Experimentally, we are most sensitive to these anomalies by measuring the invariant diboson mass or the photon transverse momentum distribution; an example is given in Figure 1 for Zγ production where the sensitivity is strongly dependent on the form factor scale. W/Z + photon processes have a clean signature and a sufficiently large cross section in pp collisions to allow for precision measurements. Background sources are limited and can be suppressed by an appropriate event selection. Misidentified, isolated photons from the decay of neutral meson in W/Z+jet events are the main background source in the Tevatron experiments, CDF and DØ. The probabilty that a jet fragments into a neutral meson which is then mistakenly detected as a single photons is very small at high jet energies. At CMS and ATLAS such QCD background contributions are therefore less problematic and can be assumed to be negligible for photon P_T's above approximately 100 GeV. In this region, anomalous gauge boson couplings would be most pronounced.

Unlike at the Tevatron experiments, we have to pay attention to pronounced QCD contributions to the Wγ/Zγ cross section at LHC energies. Already next-to-leading order (NLO) corrections enhance the Standard Model cross section particularly at high photon P_T (Figure 2) and therefore would reduce the sensitivity to anomalous couplings if not properly taken into account. However, as NLO weak boson + photon events are usually characterized by the presence of one or more high momentum jets, vetoing events containing at least one high P_T jet significantly

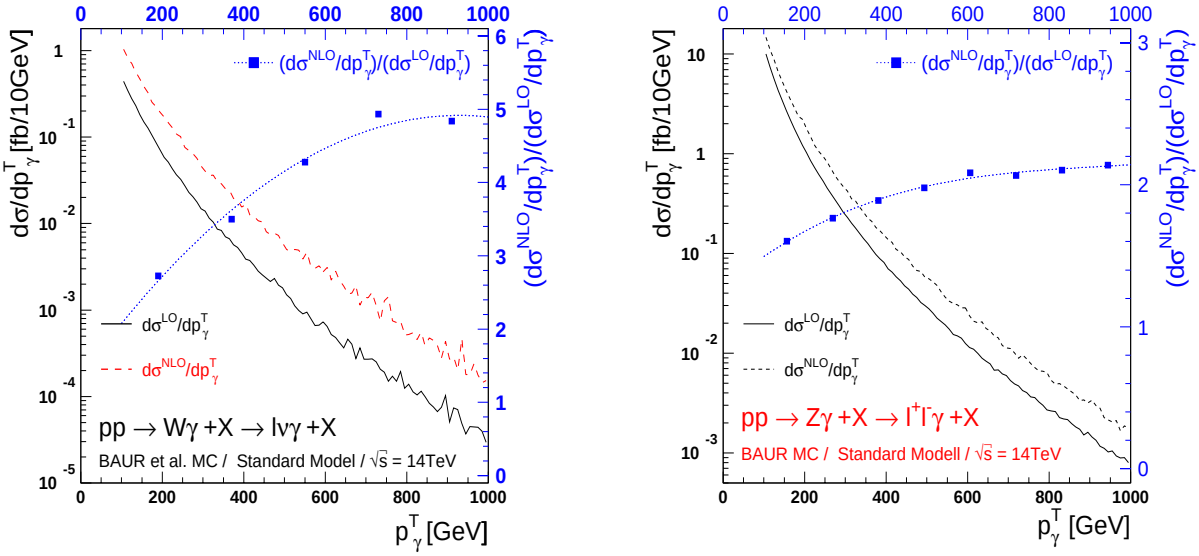

Figure 2: NLO QCD contributions in Wγ and Zγ production.

suppresses such NLO contributions. Additionally, unwanted uncertainties in the differential NLO Wγ/Zγ + X cross sections due to variations of the factorization scale are avoided through the use of a *jet veto* [8, 9].

3 Event Selection

Our study includes only the electron and muon decay channels of the W and Z bosons. A similar analysis using hadronic weak boson decays should be possible but would require elaborate QCD background studies.

Another mode, $pp \to (Z \to \nu\bar{\nu}) + \gamma$, is also not included in this analysis despite the Z boson's large branching ratio into a neutrino pair. Although the $Z \to \nu\bar{\nu}$ cross section is approximately a factor of three larger than the electron and muon channels combined, the need to suppress strong backgrounds from dijet and direct photon production will drastically reduce the Zγ detection efficiency. Such an analysis requires a good understanding of the missing transverse energy reconstruction in the appropriate data sets, which has not been done at CMS so far.

The event selections in the Wγ and Zγ channels are very simliar. The signature consists of a high P_T lepton and a well isolated photon. The additional presence of a second charged lepton or large missing energy defines the Z or W boson, respectively.

To subtract radiative events where the photon is emmitted off of a charged decay lepton, the photon is required to be well separated and to form together with the leptons a mass greater than that of the decaying boson: the photon-lepton separation, defined in the rapidity-azimuth space as $\Delta R_{\ell\gamma} = \sqrt{\Delta\phi_{\ell\gamma}^2 + \Delta\eta_{\ell\gamma}^2}$, is required to be larger than 0.7; the invariant Zγ mass must exceed 100 GeV/c^2 and the invariant transverse mass of the Wγ system (cluster transverse mass) must be larger than 90 GeV/c^2. The Wγ cluster transverse mass is defined as

Pseudorapidity Photon/Lepton	$\lvert\eta_{\gamma/\ell}\rvert < 2.4$
Transverse Energy Photon	$P_{T,\gamma} > 100\,\mathrm{GeV}$
Transverse Energy Lepton	$P_{T,\ell} > 25\,\mathrm{GeV}$
Photon-Lepton Separation	$\Delta R_{\ell\gamma} > 0.7$
Missing Energy	$\not\!\!E_T > 50\,\mathrm{GeV}$
Wγ Cluster Transverse Mass	$M_{TC}^{W\gamma} > 90\,\mathrm{GeV/c^2}$
Zγ Three-body Mass	$M_{\ell\ell\gamma} > 100\,\mathrm{GeV/c^2}$

Table 1: Summary of W and Z selection requirements.

$$M_{TC}^{W\gamma} = \sqrt{\left[\left(M_{\ell\gamma}^2 + \left|\vec{P}_T^{\,\gamma} + \vec{P}_T^{\,\ell}\right|^2\right)^{\frac{1}{2}} + \left|\vec{P}_T^{\,\bar{\nu}_\ell}\right|\right]^2 - \left|\vec{P}_T^{\,\gamma} + \vec{P}_T^{\,\ell} + \vec{P}_T^{\,\bar{\nu}_\ell}\right|^2}, \quad (9)$$

where $M_{\ell\gamma}^2$ is the invariant mass of the electron-photon pair and $\vec{P}_T^{\,\gamma}$ ($\vec{P}_T^{\,\ell}$, $\vec{P}_T^{\,\bar{\nu}_\ell}$) is the transverse momentum vector of the photon (lepton, antineutrino). Table 1 displays a summary of the weak boson and photon selection requirements used in this analysis.

We use Pythia 6.1 [10] to obtain a more realistic fragmentation of the generated partons in the detector volume. As the event generators produce flavor- and color-averaged results, it is not possible to assign color to a quark jet. Because of that, we use gluon jets in the Pythia fragmentation. We generated "data sets" in which NLO contributions are suppressed by imposing a jet veto: events with a jet of $P_{T\,jet} > 50\,\mathrm{GeV}$ within $|\eta_{jet}| < 3.0$ are discarded.

4 Event Simulation

We used the *Baur et al.* NLO Wγ [8] and Zγ [9] event generators. The NLO calculations include contributions from the square of the Born graphs, interferences between Born graphs and virtual one-loop diagrams, and the square of the real emissions graph. At leading-logarithm level, bremsstrahlung processes from a final state quark are included in addition to the lowest order diagrams, representing VVγ (V = W, Z) production.

The programs employ a combination of analytic and Monte Carlo integration techniques [11]. Soft and collinear singularities associated with the real emission subprocesses are isolated by partitioning the phase space into soft, collinear, and finite regions. Details about these techniques can be found in [8, 9, 12]. Important for this analysis is the fact that extremely large event weights occur due to the singularities. These large weights are rare, but their presence requires the generation of high statistics samples to avoid strong local fluctuations in the differential cross section distributions. In praxis, the size of a data sample is limited if one requires a reasonable processing time by the detector simulation. We found that the generation of data sets of the order of one million events is a good compromise; the physics distributions are sufficiently smooth and the processing time is in the order of half a day on a typical PII(400MHz) or Alpha (433MHz) machine.

We used CMSJET 4.7-WγZ as a parameterized CMS detector simulation. CMSJET 4.7-WγZ differs from the default CMSJET 4.7 [13] in the definitions of calorimetry and track isolation. In Zγ events containing a ZZγ vertex, a high P_T photon typically concurs with a high P_T Z boson which decays in a dilepton pair with predominantly small angular separation. The track isolation in CMSJET 4.7, however, does not allow a charged particle of $P_T > 2\,\mathrm{GeV}$ within a radius $R \leq 0.3$ around a reconstructed track. To retain sensitivity to anomalous couplings, we reject in CMSJET 4.7-WγZ events only when a second charged particle within the cone of $R \leq 0.3$ falls in the region $2 < P_T < 50\,\mathrm{GeV}$. Similarly, the calorimeter isolation requirement, the total EM energy in a ring $0.05 < R < 0.3$ around the center-of-gravity in particle cluster with radius $R < 0.5$, was required to be less than 2 GeV. In CMSJET 4.7-WγZ, we exclude in this energy summation clusters (with size $R < 0.05$) which correspond to a track with $P_T > 50\,\mathrm{GeV}$. With this modifications, we are able to keep events where a charged lepton with $P_T > 50\,\mathrm{GeV}$ borders, but does not overlap with the another charged, high P_T lepton

In the actual CMS data analysis, the observed data should contain small amounts of background [14,15]. However, this background is expected to be very small at high photon energies and is assumed to be negligible in our study of excess events in the tail of the photon P_T distribution.

5 Sensitivity Study

To extract sensitivities on anomalous couplings at CMS, we performed a binned maximum likelihood fit to the transverse momentum distribution of the photon in Wγ and Zγ events. For such a study, it is necessary to investigate a large number of different sets of couplings. Fortunately, it is not necessary to run the Monte Carlo simulation for each of these sets. The cross section can be expressed analytically by a quadratic function of these couplings,

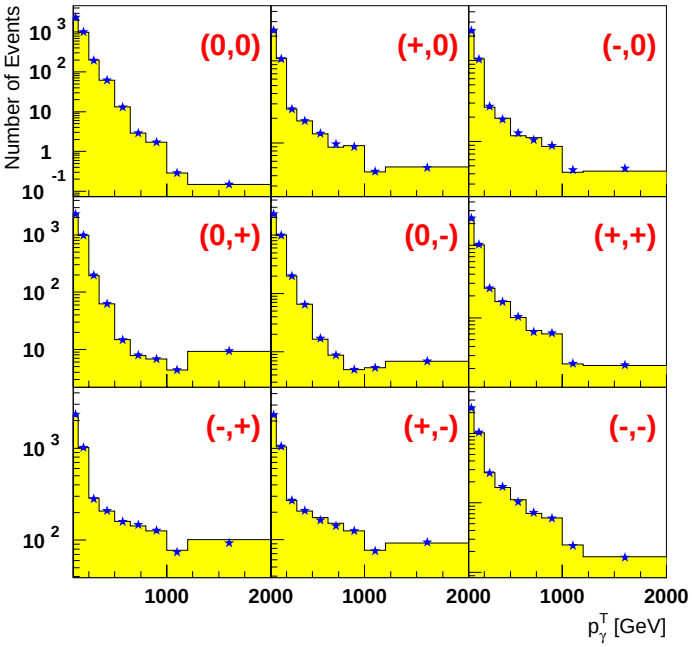

Figure 3: Photon P_T distribution for nine Zγ data sets. Each set was generated for a coupling pair (h_{30}^Z,h_{40}^Z). With the numerical values $h_{30}^Z = (\pm 4 \cdot 10^{-3}, 0)$ and $h_{40}^Z = (\pm 3.5 \cdot 10^{-6}, 0)$, we obtain nine different combinations, symbolically labeled as (0,0), (+,0) etc. The prediction from a fit to these curves reproduces the data in each P_T interval well ($\star$).

since the Wγ and Zγ amplitudes are linear in the anomalous coupling parameters. Hence, the number of predicted Wγ or Zγ events for a given coupling pair (ac_1, ac_2) is given by an elliptical paraboloid with six coefficients:

$$N_i^{pred}(ac_1, ac_2) = N_i^{SM} + A_i \cdot ac_1 + B_i \cdot ac_2 + C_i \cdot ac_1^2 + D_i \cdot ac_2^2 + E_i \cdot ac_1 \cdot ac_2, \qquad (10)$$

where ac_1 and ac_2 is to be substituted by $\Delta\kappa$ or h_{30}^Z, and λ or h_{40}^Z, respectively.

The six coefficients were determined in each transverse photon energy interval by fitting the paraboloid to nine Monte Carlo samples for the following combinations of some arbitrary coupling values AC1 and AC2 [2)]: (AC1, AC2) (0,AC2) (-AC1,AC2) (AC1,0) (0,0) (-AC1, 0) (AC1,-AC2) (0,-AC2) (-AC1,-AC2). With that information, we were able to predict the number of events in a given photon P_T bin for *any* pair (ac_1, ac_2).

We chose to divide the photon P_T distribution into nine bins with variable width[3)] As an example, Figure 5 show that after the six coefficients were obtained through the fit of Zγ photon P_T distributions, the number of events in each bin are reasonably well predicted by (10). We estimated the CMS sensitivity to detect anomalies by comparing the binned photon P_T distributions for various anomalous coupling pairs to data expected to be measured by CMS in the case of Standard Model couplings. The expected data set was simulated by Poisson-fluctuating the predicted number of events for each bin of the Standard Model photon P_T distribution after the CMS detector simulation in order to account for statistical variations in the experiment.

We calculated the likelihood that the data corresponding to anomalous couplings are consistent with Standard Model data using Poisson statistics. Defining a confidence level (CL), we then determined the region of the coupling parameter space in which we will be sensitive to anomalies with the CMS experiment. The analysis method will be described in the following.

[2)] In praxis, these numbers should be close to the expected sensitivities to reduce uncertainties in the fit.

[3)] While it may seem necessary to use the overall shape information for the comparison, it is sufficient to divide the P_T distributions into distinct bins; the absolute number of excess events in the tail dominates in the statistical analysis. An unbinned fit method would require a precise knowledge of the background behavior as a function of photon P_T. It would also requires, due to the large generator weights, the generation of high statistics Monte Carlo samples, ideally in the order of 10 millions.

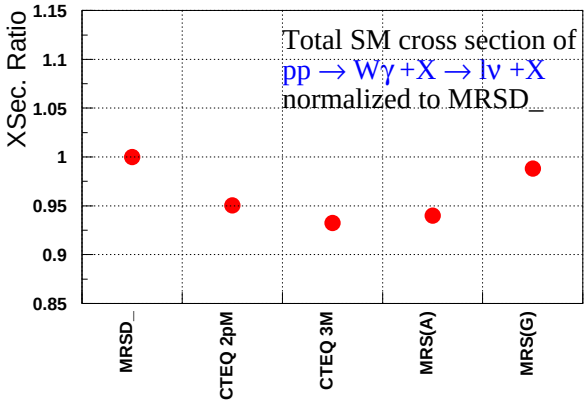

Figure 4: Variation in the Wγ cross section prediction due to the choice the parton density function.

For a given bin i, the probability for measuring the Standard Model prediction N_i^{sm} when N_i^{ac} events for a particular coupling pair (ac_1, ac_2) are observed is given by:

$$\mathcal{P}_i = \frac{e^{-\mu_i} \cdot \mu_i^{N_i^{ac}}}{N_i^{ac}!}, \tag{11}$$

with $\mu_i = N_i^{sm}$.

The likelihood function is then defined as the product of the individual probabilities over all bins:

$$\mathcal{L}(\Delta\kappa, \lambda) = -ln \int_{-\infty}^{+\infty} \prod_{i}^{nbins} \frac{e^{-\mu_i + sys_i(x)} \cdot (\mu_i + sys_i(x))^{N_i^{ac}}}{N_i^{ac}!} \cdot G(x)\ dx. \tag{12}$$

To account for systematic uncertainties $sys_i(x)$, a Gaussian probability density G(x) is folded in. The integration was performed by simulating 90 different CMS experiments, in each of which the nominal number of events $\mu_i + sys_i(x)$ is changed by a fraction.

We conservatively assumed an overall error of 20%, mainly due to uncertainties in the luminosity ($\sim 10\%$) [4], in the shape of the generated transverse momentum distribution of the diboson system, the choice of the four-momentum Q^2 of the intermediate weak boson, the choice of the parton density function (Figure 4), the difference between the parameterized CMSJET and a detailed detector simulation (altogether $\sim 10\%$), in the efficiency and acceptance determination ($\sim 5\%$), and in the background estimate ($\sim 10\%$). A smaller value changes the results only slightly. For example, the coupling limits improve by less than 10% if a total uncertainty of 10% is assumed [16].

To find the maximum likelihood as a function of anomalous couplings, the two-dimensional space spanned by the $\mathcal{CP}$-conserving couplings is scanned. There is no a priori reason why the remaining couplings should not differ from their Standard Model value at the same time. However, to be able to display the sensitivity curves and assuming $\mathcal{CP}$-conservation, only two couplings are allowed to be anomalous.

In a two-dimensional coupling space, the sensitivity limits extracted from the log likelihood curves form an ellipses for a particular confidence level. Figure 5 shows the Wγ and Zγ contours for the 68%, 90%, and 95% CL, corresponding to a negative log likelihood value of 1.15, 2.3, 3.0, respectively. They were obtained for an energy scale of $\Lambda = 10\,\mathrm{TeV}$ (Wγ) and $\Lambda = 6\,\mathrm{TeV}$ (Zγ); a jet veto was applied to both "data samples". Curves for other scales and integrated luminosities are included in Appendix B

Our sensitivity on finding anomalous couplings are dependent on the scale where new physics would set in. This can be understood by the fact, that at such a cut-off scale the cross section of diboson production is suppressed by the form factor behavior in order to preserve unitarity; the smaller the scale, the less enhanced the cross section in presence of anomalous couplings will be. The finite center-of-mass energy restricts the accessible form factor scale to a certain (asymptotical) value, which defines the maximal discovery potential.

[4] While CMS hopes to achieve a precision of 5% or less, we assume based on the experience at the Tevatron that the luminosity will not be known much better than $\mathcal{O}(10\%)$ in the first years of LHC operation.

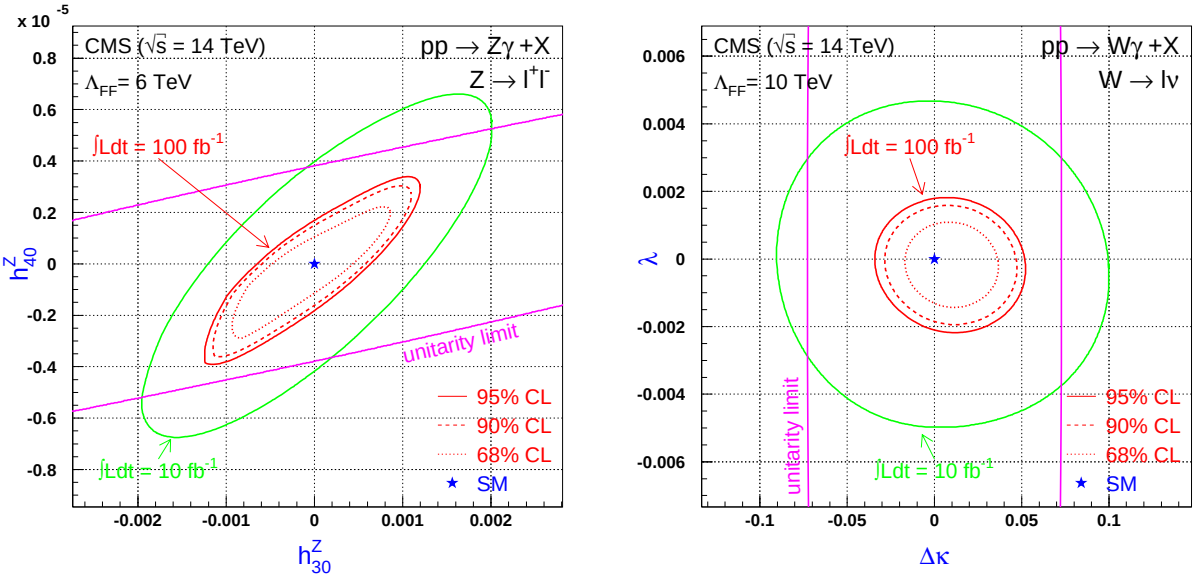

Figure 5: Sensitivity contours in the $\mathcal{CP}$-conserving WWγ and ZZγ coupling space.

At the LHC the cross section enhancement is much more pronounced than at the Tevatron, particularly for Zγ production. Form factor scales up to $10\,\mathrm{TeV}$ (Wγ) and $6\,\mathrm{TeV}$ (Zγ) will be accessible, as shown in Figures 6 and 7. For higher scales, the sensitivity remains essentially constant. Also included in these figures are the unitarity limits which define the maximum possible cut-off scale for a given anomalous coupling.

It is common to quote one-dimensional limits. We define them as the intersection points of the ellipses with the coordinate axis. At this point the three other couplings are equal to their Standard Model value of zero.

At 95% CL, we find for an integrated luminosity of $100\mathrm{fb}^{-1}$:

W-Photon couplings ($\Lambda_W = 10$ TeV) :

$$\begin{array}{rcccll} -3.4\cdot10^{-2} & < & \Delta\kappa & < & 5.2\cdot10^{-2} & \text{for} \quad \lambda = 0 \\ -2.1\cdot10^{-3} & < & \lambda & < & 1.8\cdot10^{-3} & \text{for} \quad \Delta\kappa = 0 \end{array}$$

Z-Photon couplings ($\Lambda_Z = 6$ TeV) :

$$\begin{array}{rcccll} -6.5\cdot10^{-4} & < & h_{30}^Z & < & 6.4\cdot10^{-4} & \text{for} \quad h_{40}^Z = 0 \\ -1.8\cdot10^{-6} & < & h_{40}^Z & < & 1.7\cdot10^{-6} & \text{for} \quad h_{30}^Z = 0 \end{array}$$

$W^\pm\gamma \to \ell^\pm\nu\gamma$, $\int \mathcal{L}\,dt = 10\,\mathrm{fb}^{-1}$, $\Lambda = 10$ TeV		
Baur et al. (only $W^+ \to \ell^+\nu$) [17]	$\lvert\Delta\kappa\rvert < 2\cdot10^{-1}$	$\lvert\lambda\rvert < 1\cdot10^{-2}$
this study	$\lvert\Delta\kappa\rvert < 1\cdot10^{-1}$	$\lvert\lambda\rvert < 5\cdot10^{-3}$
$Z\gamma \to \ell^+\ell^-\gamma$, $\int \mathcal{L}\,dt = 100\,\mathrm{fb}^{-1}$, $\Lambda = 3$ TeV		
Baur et al. [9]	$\lvert h_{30}^Z\rvert < 3\cdot10^{-3}$	$\lvert h_{40}^Z\rvert < 2\cdot10^{-5}$
this study	$\lvert h_{30}^Z\rvert < 1\cdot10^{-3}$	$\lvert h_{40}^Z\rvert < 1\cdot10^{-5}$

Table 2: Comparison of CMS sensitivities to anomalous gauge boson couplings at 95% CL obtained in this analysis with previous studies where no realistic detector simulation was used. Note that in contrast to this study, *maximal* bounds (i.e. not taken at the axis intersection where the second coupling vanishes) are quoted in [9] and [17].

$W^{\pm}\gamma \to \ell^{\pm}\nu\gamma$			
LEPII (combined [18])	n/a	$-7 \cdot 10^{-2} < \Delta\kappa < 3 \cdot 10^{-1}$	$-1 \cdot 10^{-1} < \lambda < 3 \cdot 10^{-2}$
Tevatron (DØ [2])	2 TeV	$-3 \cdot 10^{-1} < \Delta\kappa < 4 \cdot 10^{-1}$	$-2 \cdot 10^{-1} < \lambda < 2 \cdot 10^{-1}$
LHC (CMS, this study)	10 TeV	$-3 \cdot 10^{-2} < \Delta\kappa < 5 \cdot 10^{-2}$	$-2 \cdot 10^{-3} < \lambda < 2 \cdot 10^{-3}$
$Z\gamma \to \ell^{+}\ell^{-}\gamma$			
LEPII (L3 [5])	n/a	$\lvert h_{30}^{Z}\rvert < 2 \cdot 10^{-1}$	$\lvert h_{40}^{Z}\rvert < 3 \cdot 10^{-1}$
Tevatron (DØ [3])	0.75 TeV	$\lvert h_{30}^{Z}\rvert < 4 \cdot 10^{-1}$	$\lvert h_{40}^{Z}\rvert < 5 \cdot 10^{-2}$
LHC (CMS, this study)	10 TeV	$\lvert h_{30}^{Z}\rvert < 7 \cdot 10^{-4}$	$\lvert h_{40}^{Z}\rvert < 2 \cdot 10^{-6}$

Table 3: Comparison of CMS sensitivities to anomalous gauge boson couplings obtained in this analysis with present measurements at 95% CL.

The Tables 4 and 5 in Appendix A summarize the sensitivities on the anomalous Wγ and Zγ couplings at various confidence levels and for different energy scales. Our results are in close agreement with those obtained in a first study of Wγ and Zγ production at the LHC by [9, 17] (Table 2). The authors, however, did not utilize a realistic CMS detector simulation, and—in the case of Wγ production—restricted their analysis to the $W^{+} \to \ell^{+}\nu$ channel for a LHC center-of-mass energy of $17\,\mathrm{TeV}$.

Present measurement of anomalous WWγ and ZZγ parameters at LEPII and the Tevatron are in the order of a few 10^{-1} (Table 3). Our studies show that due to the strong increase of anomalous contributions at high center-of-mass energy, CMS will able to probe the trilinear gauge sector of electroweak interactions with significantly improved sensitivities, already with an integrated luminosity of $100\,\mathrm{fb}^{-1}$, which is equivalent to one year of expected LHC high luminosity operation. While CMS will be numerically competitive with present LEPII results on the WWγ coupling $\Delta\kappa$, an order of magnitude better sensitivity in measuring λ will be possible. The improvement for ZZγ couplings in the order of $10^{3} - 10^{5}$ will be particularly strong. Additionally, weak boson structures corresponding to energy scales up to 10 TeV will be accessible at the LHC.

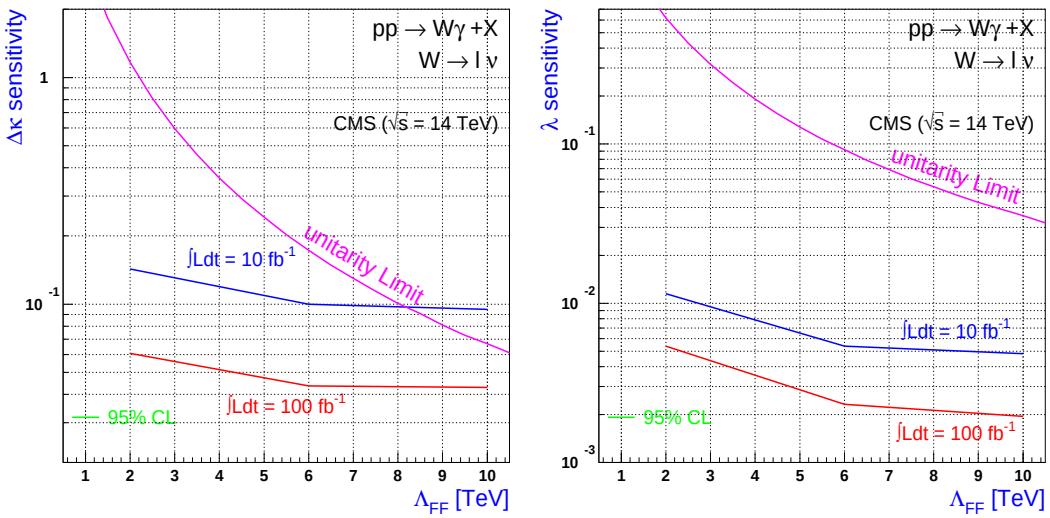

Figure 6: Sensitivities on the $\mathcal{CP}$-conserving Wγ couplings as a function of the cut-off scale.

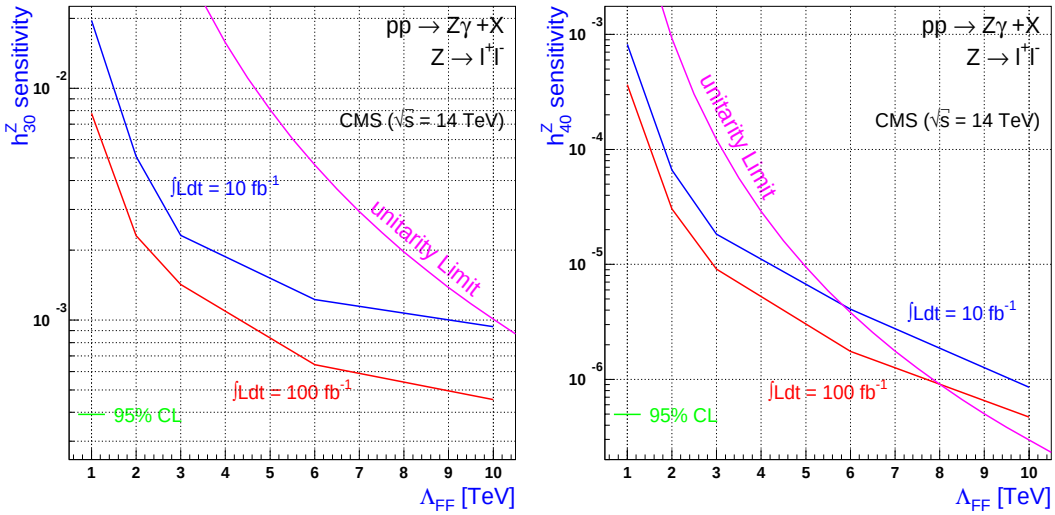

Figure 7: Sensitivities on the $\mathcal{CP}$-conserving Zγ couplings as a function of the cut-off scale.

References

[1] F. Abe *et al.* (CDF Collaboration), Phys. Rev. Lett. 74, 1936 (1995), Phys. Rev. Lett. 74, 1941 (1995), Phys. Rev. Lett. 75, 1017 (1995), Phys. Rev. Lett. 78, 4536 (1997); S. Abachi *et al.* (DØ Collaboration), Phys. Rev. Lett. 75, 1034 (1995); Phys. Rev. D 56, 6742 (1997), Phys. Rev. Lett. 78, 3634 (1997), Phys. Rev. Lett. 75, 1028 (1995), Phys. Rev. Lett. 75, 3640 (1997), Phys. Rev. Lett. 56, 6742 (1997), Phys. Rev. Lett. 75, 1023 (1995), Phys. Rev. Lett. 77, 3303 (1996), Phys. Rev. Lett. 79, 1441 (1997), Phys. Rev. D 57, 3817 (1998).

[2] B. Abbott *et al.* (DØ Collaboration), Phys. Rev. D 58, 3102 (1998).

[3] M. Acciarri *et al.* (DØ Collaboration), Phys. Lett. B 467, 171 (1999).

[4] R. Barate *et al.* (ALPEPH Collaboration), Phys. Lett. B 422, 369 (1998), ALEPH 99-072 CONF 99-046, ALEPH 99-072 CONF 99-028; P. Abreu *et al.* (DELPHI Collaboration), Phys. Lett. B 423, 194 (1998), DELPHI 99-63 CONF 250, Phys. Lett. B 459, 382 (1999); M. Acciarri *et al.* (L3 Collaboration), Phys. Lett. B 403, 168 (1997), Phys. Lett. B 407, 419 (1997), Phys. Lett. B 413, 176 (1997), Phys. Lett. B 436, 187 (1998), Phys. Lett. B 436, 417 (1998), Phys. Lett. B 465, 363 (1999), Phys. Lett. B 467, 171 (1999); K. Ackerstaff *et al.* (OPAL Collaboration), Phys. Lett. B 397, 147 (1997), Eur. Phys. J. C2, 597 (1998); G. Abbiendi *et al.* (OPAL Collaboration), Eur. Phys. J. C8, 191 (1999), Phys. Lett. B 471, 293 (1999).

[5] L3 Collaboration, Internal Note 2513, submitted to the 2000 Moriond Conference; see also: DELPHI Collaboration, 2000-028 CONF 347, submitted to the 2000 Moriond Conference

[6] R.W. Brown *et al.*, Phys. Rev. D 20, 116 (1979) , K.O. Mikaelian *et al.* Phys. Rev. Lett. 43, 746 (1979).

[7] J. Ellison and J. Wudka, Annu. Rev. Nucl. Part. Sci. 48, 33 (1998).

[8] U. Baur, T. Han, and J. Ohnemus, Phys. Rev. D 48, 5140 (1993).

[9] U. Baur, T. Han, and J. Ohnemus, Phys. Rev. D 57, 2823 (1998).

[10] T. Sjöstrand, Comput. Phys. Commun., 82 (1994).

[11] H. Baer, J. Ohnemus, and J.F. Owens, Phys. Rev. D 40, 2844 (1989); H. Baer, J. Ohnemus, and J.F. Owens, Phys. Rev. D 42, 61 (1990); Phys. Lett. B 234, 127 (1990); J. Ohnemus, J.F. Owens, Phys. Rev. D 43, 3627 (1991); J. Ohnemus, Phys. Rev. D 44, 1403 (1991); J. Ohnemus, Phys. Rev. D 44, 3477 (1991); H. Baer and M.H. Reno Phys. Rev. D 43, 2892 (1991), H. Bailey, J. Ohnemus, and J.F. Owens, Phys. Rev. D 46, 2018 (1992), J. Ohnemus, Phys. Rev. D 47, 940 (1993); J. Ohnemus and W.J. Stirling, Phys. Rev. D 47, 2722 (1993), H. Baer, H. Bailey, and J.F. Owens, Phys. Rev. D 47, 2730 (1993).

[12] G.'t Hooft and M. Veltman, Nucl.Phys. B44, 189 (1972); U. Baur, E.W.N. Glover, and J.J. van der Bij, Nucl. Phys. B318, 106 (1989); V. Barger, T. Han, J. Ohnemus, and D. Zeppenfeld, Phys. Rev. D 41, 2782 (1990).

[13] S. Abdullin, A Khanov, and N. Stephanov, CMS TN/94-180 (1999).

[14] ATLAS Collaboration, ATALS Technical Proposal, ATL-PHYS-94-060 (1994).

[15] C.K. Mackay, 'The electromagnetic calorimeter for CMS and a study of the WWγ vertex', Brunel University, Uxbridge, UK, CMS/1999-012THESIS, RAL-TH-1999-001 (1999).

[16] M. Reischl, 'Simulationsstudien zur Wγ Produktion in hadronischen Kollisionen bei CDF und CMS', Diplomarbeit, Universität Karlsruhe, Germany, IEKP-KA/98-6 (1998).

[17] U. Baur and D. Zeppenfeld, Nucl.Phys. B 308, 127 (1988).

[18] The LEP Collaborations ALEPH, DELPHI, L3, OPAL, the LEP Electroweak Working Group, and the SLD Heavy Flavour and Electroweak Groups, CERN-EP-2000-016 (2000).

A Summary of Sensitivities

Λ [TeV]	$\int \mathcal{L}\,dt = 10\,\text{fb}^{-1}$			$\int \mathcal{L}\,dt = 100\,\text{fb}^{-1}$		
2	$-0.13 <$	$\Delta\kappa$	< 0.15	$-6.0 \cdot 10^{-2} <$	$\Delta\kappa$	$< 6.2 \cdot 10^{-2}$
	$-1.1 \cdot 10^{-2} <$	λ	$< 1.2 \cdot 10^{-2}$	$-5.8 \cdot 10^{-3} <$	λ	$< 5.0 \cdot 10^{-3}$
6	$-9.5 \cdot 10^{-2} <$	$\Delta\kappa$	$< 10.4 \cdot 10^{-2}$	$-4.0 \cdot 10^{-2} <$	$\Delta\kappa$	$< 4.7 \cdot 10^{-2}$
	$-5.5 \cdot 10^{-3} <$	λ	$< 5.2 \cdot 10^{-3}$	$-2.5 \cdot 10^{-3} <$	λ	$< 2.2 \cdot 10^{-3}$
10	$-9.0 \cdot 10^{-2} <$	$\Delta\kappa$	$< 10.0 \cdot 10^{-2}$	$-3.4 \cdot 10^{-2} <$	$\Delta\kappa$	$< 5.2 \cdot 10^{-2}$
	$-5.0 \cdot 10^{-3} <$	λ	$< 4.7 \cdot 10^{-3}$	$-2.1 \cdot 10^{-3} <$	λ	$< 1.8 \cdot 10^{-3}$

Table 4: Sensitivities for $\mathcal{CP}$-conserving Wγ couplings at CMS for various form factor scales, Λ, and integrated luminosities, $\int \mathcal{L}\,dt$. The values quoted are taken at the intersection of the two-dimensional contours (see Appendix B) with the axes, where all other coupling parameters equal their Standard Model value.

Λ [TeV]	$\int \mathcal{L}\,dt = 10\,\text{fb}^{-1}$			$\int \mathcal{L}\,dt = 100\,\text{fb}^{-1}$		
1	$-2.0 \cdot 10^{-2} <$	h_{30}^Z	$< 2.0 \cdot 10^{-2}$	$-7.8 \cdot 10^{-3} <$	h_{30}^Z	$< 7.8 \cdot 10^{-3}$
	$-8.3 \cdot 10^{-4} <$	h_{40}^Z	$< 8.2 \cdot 10^{-4}$	$-3.7 \cdot 10^{-4} <$	h_{40}^Z	$< 3.6 \cdot 10^{-4}$
2	$-5.2 \cdot 10^{-3} <$	h_{30}^Z	$< 5.0 \cdot 10^{-3}$	$-2.4 \cdot 10^{-3} <$	h_{30}^Z	$< 2.2 \cdot 10^{-3}$
	$-6.4 \cdot 10^{-5} <$	h_{40}^Z	$< 6.8 \cdot 10^{-5}$	$-2.9 \cdot 10^{-5} <$	h_{40}^Z	$< 3.2 \cdot 10^{-5}$
3	$-2.3 \cdot 10^{-3} <$	h_{30}^Z	$< 2.3 \cdot 10^{-3}$	$-1.5 \cdot 10^{-3} <$	h_{30}^Z	$< 1.4 \cdot 10^{-3}$
	$-1.9 \cdot 10^{-5} <$	h_{40}^Z	$< 1.8 \cdot 10^{-5}$	$-9.7 \cdot 10^{-6} <$	h_{40}^Z	$< 8.5 \cdot 10^{-6}$
6	$-1.2 \cdot 10^{-3} <$	h_{30}^Z	$< 1.3 \cdot 10^{-3}$	$-6.5 \cdot 10^{-4} <$	h_{30}^Z	$< 6.4 \cdot 10^{-4}$
	$-4.2 \cdot 10^{-6} <$	h_{40}^Z	$< 4.0 \cdot 10^{-6}$	$-1.8 \cdot 10^{-6} <$	h_{40}^Z	$< 1.7 \cdot 10^{-6}$

Table 5: Sensitivities for $\mathcal{CP}$-conserving Zγ couplings at CMS for various form factor scales, Λ, and integrated luminosities, $\int \mathcal{L}\,dt$. The values quoted are taken at the intersection of the two-dimensional contours (see Appendix B) with the axes, where all other coupling parameters equal their Standard Model value.

B Summary of Sensitivity Contours

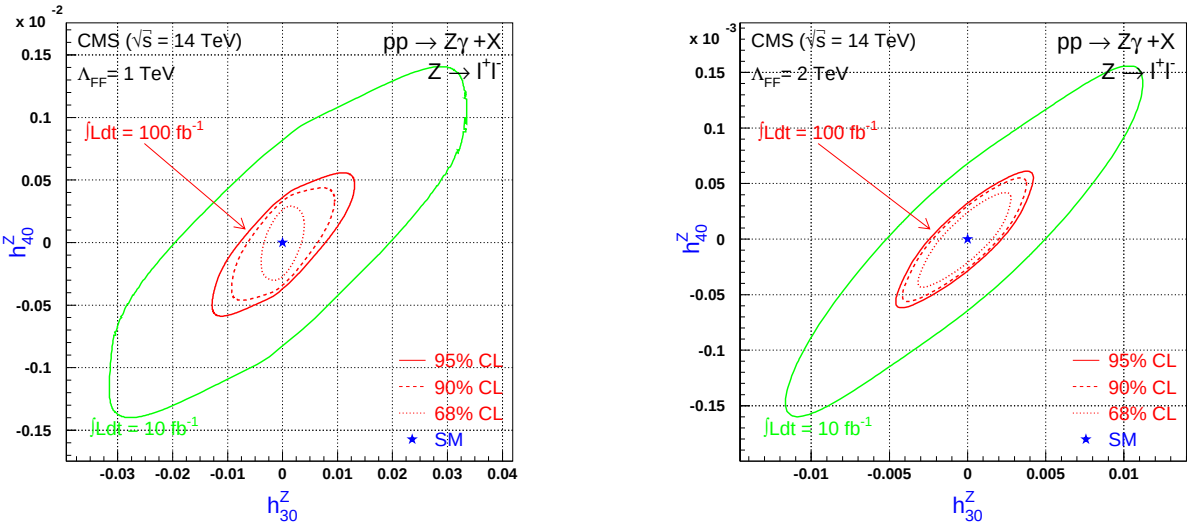

Figure 8: CMS sensitivity contours in the $\mathcal{CP}$-conserving Zγ coupling space for $\Lambda = 1$ TeV and $\Lambda = 2$ TeV.

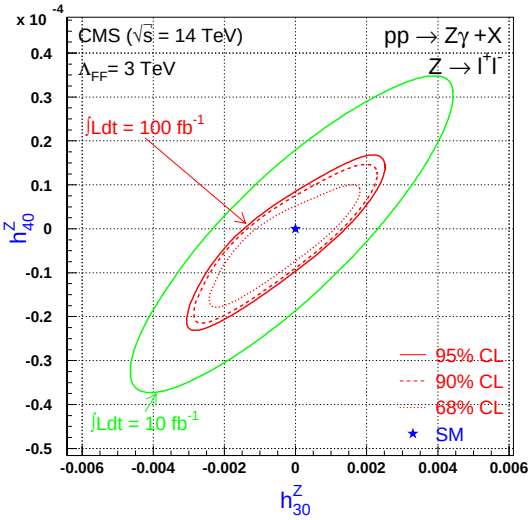

Figure 9: CMS sensitivity contours in the $\mathcal{CP}$-conserving Zγ coupling space for $\Lambda = 3$ TeV.

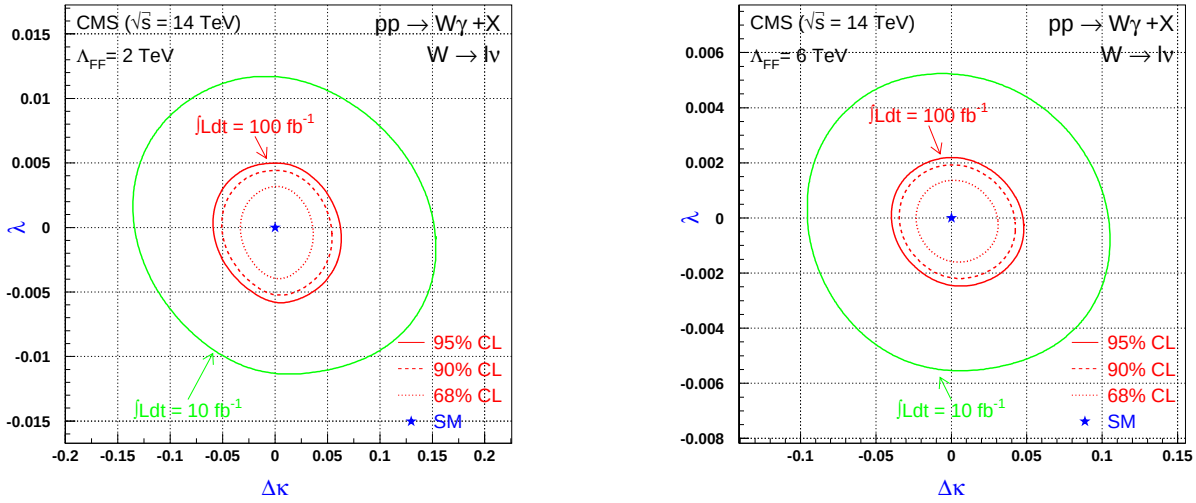

Figure 10: CMS sensitivity contours in the $\mathcal{CP}$-conserving Wγ coupling space for $\Lambda = 2$ TeV and $\Lambda = 6$ TeV.